HHS Public Access

Author manuscript

Neurogastroenterol Motil. Author manuscript; available in PMC 2018 May 01.

Published in final edited form as:

Neurogastroenterol Motil. 2017 May ; 29(5): . doi:10.1111/nmo.13010.

High-resolution electrical mapping of porcine gastric slow-wave propagation from the mucosal surface

Timothy R. Angeli[1], **Peng Du**[1], **Niranchan Paskaranandavadivel**[1], **Shameer Sathar**[1], **Andrew Hall**[2], **Samuel J. Asirvatham**[3], **Gianrico Farrugia**[4], **John A. Windsor**[2], **Leo K. Cheng**[1,5], and **Gregory O'Grady**[1,2]

[1] Auckland Bioengineering Institute, University of Auckland, New Zealand. [2] Department of Surgery, University of Auckland, New Zealand. [3] Division of Cardiovascular Diseases, Mayo Clinic, Rochester, MN, USA. [4] Department of Gastroenterology and Hepatology, Mayo Clinic, Rochester, MN, USA. [5] Department of Surgery, Vanderbilt University, Nashville, TN, USA.

Abstract

Background—Gastric motility is coordinated by bioelectrical slow-waves, and gastric dysrhythmias are reported in motility disorders. High-resolution (HR) mapping has advanced the accurate assessment of gastric dysrhythmias, offering promise as a diagnostic technique. However, HR mapping has been restricted to invasive surgical serosal access. This study investigates the feasibility of HR mapping from the gastric mucosal surface.

Methods—Experiments were conducted *in-vivo* in 14 weaner pigs. Reference serosal recordings were performed with flexible-printed-circuit (FPC) arrays (128-192 electrodes). Mucosal recordings were performed by two methods: 1) FPC array aligned directly opposite the serosal array, and 2) cardiac mapping catheter modified for gastric mucosal recordings. Slow-wave propagation and morphology characteristics were quantified and compared between simultaneous serosal and mucosal recordings.

Key Results—Slow-wave activity was consistently recorded from the mucosal surface from both electrode arrays. Mucosally-recorded slow-wave propagation was consistent with reference serosal activation pattern, frequency ($P \geq 0.3$), and velocity ($P \geq 0.4$). However, mucosally-recorded slow-wave morphology exhibited reduced amplitude (65-72% reduced, $P < 0.001$) and wider downstroke width (18-31% wider, $P \leq 0.02$), compared to serosal data. Dysrhythmias were successfully mapped and classified from the mucosal surface, accorded with serosal data, and were consistent with known dysrhythmic mechanisms in the porcine model.

Corresponding Author (and address for reprints): A/Prof. Gregory O'Grady, Department of Surgery, University of Auckland, Private Bag 92019, Auckland, New Zealand, +64 (0)27 422 2989; greg.ogrady@auckland.ac.nz.

Author Contributions

Conception and design: TRA, LKC, GOG; collection of data: TRA, PD, NP, SS, AH, LKC; analysis, and interpretation of the data: TRA, AH, LKC, GOG; drafting of the article: TRA, GOG; critical revision of the article for important intellectual content: TRA, PD, NP, SS, AH, SJA, GF, JAW, LKC, GOG; final approval of the article: TRA, PD, NP, SS, AH, SJA, GF, JAW, LKC, GOG.

Conflict of Interest Disclosure

TRA, PD, NP, SJA, GF, LKC, and GOG hold intellectual property and/or patent applications in the field of gastrointestinal electrophysiological mapping. TRA, PD, NP, SS, JAW, LKC, and GOG hold shares in FlexiMap Ltd.

Conclusions & Inferences—HR gastric electrical mapping was achieved from the mucosal surface, and demonstrated consistent propagation characteristics with serosal data. However, mucosal signal morphology was attenuated, demonstrating necessity for optimized electrode designs and analytical algorithms. This study demonstrates feasibility of endoscopic HR mapping, providing a foundation for advancement of minimally-invasive spatiotemporal gastric mapping as a clinical and scientific tool.

Graphical Abstract

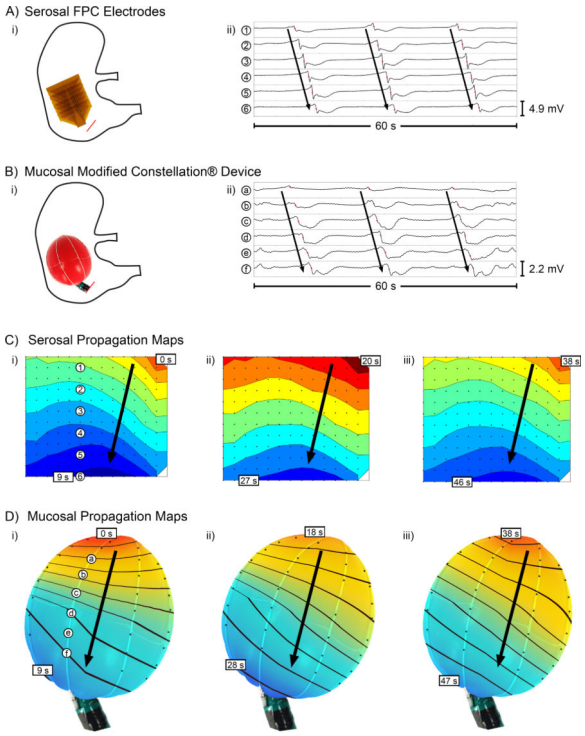

Keywords

Dysmotility; electrophysiology; endoscopy; motility; stomach

Introduction

Gastric motility is coordinated by slow-waves generated and propagated by the interstitial cells of Cajal (ICC).[1] Slow-wave dysrhythmias have been associated with gastric dysmotility, including in gastroparesis, chronic unexplained nausea and vomiting, and functional dyspepsia, and patchy ICC loss can be contributory.[2–5]

The pathophysiological significance of gastric dysrhythmias remains uncertain, and there remains no established role for their investigation and treatment in clinical practice.[6,7] A critical problem has been the lack of accurate diagnostic methods.[8,9] In recent years, however, high-resolution (HR; ‘multi-electrode’) mapping has emerged as a key advance, enabling more accurate detection, description, and classification of gastric dysrhythmias,[2,10] renewing clinical interest.[7,11]

HR mapping involves the use of dense arrays of electrodes to define slow-wave propagation sequences in fine spatiotemporal detail,[12] as commonly applied in cardiac practice.[13] The major problem in the GI field, however, has been the invasive nature of this technique, which presently requires surgical access to the serosal surface.[14] Human mapping studies, to date, have been performed under general anesthesia by laparotomy or laparoscopy.[2,15] In order to further progress research, diagnosis, and therapy of gastric dysrhythmias, it is critical to develop a minimally-invasive endoscopic approach for gastric HR mapping.

Multiple investigators over several decades have successfully recorded slow-waves at focal sites on the gastric mucosa.[16–19] However, HR mucosal recordings with spatiotemporal mapping have not yet been achieved. The aim of this study was to investigate the feasibility and potential of mapping slow-waves from the gastric mucosal surface, with comparison to simultaneous serosal mapping, in order to: 1) demonstrate proof-of-concept and feasibility of endoscopic gastric electrical mapping, 2) quantify similarities and differences between serosal and mucosal recordings, and 3) define opportunities and challenges for endoscopic mapping device design.

Methods

Animal Preparation

Ethical approval for this work was granted by the University of Auckland Animal Ethics Committee. All recordings were performed *in vivo* on fasted, cross-breed, female, weaner pigs, an established model for slow-wave investigations that exhibits spontaneous dysrhythmias during these experimental conditions, unlike humans.[20,21] General anesthesia was induced with Zoletil (Tiletamine HCl 50 mg mL^{-1} and Zolazepam HCl 50 mg mL^{-1}) and maintained with isoflurane. Vital signs were continuously monitored and maintained within the normal range throughout each study, including temperature. At the conclusion of each study, euthanasia was performed by a bolus injection of magnesium sulphate.

High Resolution Mapping Methods

Serosal reference extracellular recordings were performed using validated high-resolution flexible-printed-circuit (FPC) arrays (FlexiMap, Auckland, New Zealand), comprising 128-192 total electrodes with 0.3 mm gold contacts, in a 16 × 8-12 array with 4 mm inter-electrode spacing (**Figure 1A**).[12] For the mucosal recordings, two devices were employed: 1) the same FPC electrode array as used for serosal recordings (**Figure 1A**), and 2) a novel approach based on the cardiac Constellation™ mapping catheter (Boston Scientific, MN; 64 total electrodes, 8 x 8 flexible spherical array, 75 mm diameter, **Figure 1B,C**). The Constellation™ catheter was modified by attaching an inflatable balloon into the middle of the electrode basket (**Figure 1B**). The balloon was connected to a 140 cm long nasogastric tube, which terminated at a stop-cock connection to a 60 cm^3 syringe, allowing inflation of the device for sustained pressure of the electrodes against the mucosal surface (**Figure 1B**). Each electrode spline of the Constellation™ device was connected to the neighboring splines with flexible extruded nylon to improve the uniformity of circumferential spacing when deployed.

All pigs underwent midline laparotomy. A small transverse incision was then made through the gastric wall, either in the pre-pyloric region of the distal antrum or the fundus,[21] to allow access to the mucosal surface. For the FPC mucosal mapping studies, a 128-channel FPC electrode array (60mm × 28mm) was inserted through the incision and gently positioned against the mucosal surface of the mid-corpus. A second, identical FPC electrode array was placed on the serosal surface in close opposition to the mucosal FPC array such that both arrays were placed over the same region of the gastric corpus. Gauze packs soaked with warm saline (37°C) were packed behind the mucosal FPC array within the stomach and overlying the serosal FPC array to hold the electrodes in contact with the gastric surfaces. Recordings were obtained simultaneously from the FPC electrodes at the mucosa and serosa.

For the mucosal mapping studies using the modified Constellation™ device, it was also placed through a small incision in the gastric wall, in the same pre-pyloric (three pigs) or proximal fundal (two pigs) regions as with the FPC recordings, or through the abdominal esophagus (one pigs) to simulate endoscopic device intubation. After introduction, the device was inflated with 180 cm^3 of air (approximately 1 psi inflation pressure), and a serosal reference FPC array of 128-192 electrodes was placed on the serosa in direct opposition of the Constellation™ device, covering approximately 25% of the Constellation™ device's circumference. At the conclusion of the recording periods, the device was deflated for removal.

During all recording periods, the wound edges were approximated with clamps to minimize cooling and drying of the stomach, and ventilation was paused for occasional 30 s intervals during recordings to minimize respiratory artifacts.[14]

Data Acquisition, Signal Processing, and Analysis

Slow-wave data were acquired as mono-polar recordings via an ActiveTwo system (BioSemi, Amsterdam, The Netherlands) modified for passive recordings. Reference electrodes were placed on the hindquarter thigh, and custom software was used for the acquisition interface, written in LabView (National Instruments, TX, USA). Recordings were acquired at 512 Hz, then down-sampled to 30 Hz for analysis, prior to filtering (moving-median and Savitzky-Golay filter; effective low-pass cut-off of ~2 Hz) to remove baseline drift and high-frequency noise.[22]

Slow-wave analyses were performed using the Gastrointestinal Electrical Mapping Suite (GEMS) v1.5 (FlexiMap, Auckland, New Zealand).[23] Slow-wave activation times (ATs) were identified and clustered into propagating cycles using validated automated methods for the serosal data.[24,25] However, due to the altered morphology of mucosal signals (see results), manual placement of fiducial markers for slow-wave ATs was required for mucosal data. Slow-wave propagation patterns were then characterized by animation, and mapped as isochronal activation maps.[23] Slow-wave frequency, amplitude, and velocity were calculated using validated algorithms.[26,27] Velocity calculations from the modified Constellation™ device were performed assuming a uniform inter-electrode spacing of 11.4 mm. Slow-wave downstroke width was calculated as the time difference between the peak and trough of the slow-wave deflection,[27] and downstroke gradient was calculated as the amplitude divided by the downstroke width.

Average slow-wave signal morphologies were calculated for each of the three recording modalities (serosal FPC, mucosal FPC, and mucosal modified Constellation™), calculated from 100 representative slow-wave events across a 4 s window centered at each AT (10 signals per recording, from 10 recordings for each modality). The Pearson correlation coefficient (PCC) was then calculated between the average signals to quantify the degree of morphological correlation.[28]

Statistical Methods

Results were calculated as mean ± SD or SEM, as appropriate, and statistical comparisons were performed using Student's t-test (paired for direct serosa versus mucosa comparisons), with a significance threshold of $P < 0.05$.

Results

Data comprised a total of 20 recordings from 14 pigs (33 ± 4 kg); mucosal recordings were obtained with FPC electrodes in 10 of these recordings (8 pigs; 105 min total duration; 10.5 ± 4.0 min per recording) and from the modified Constellation™ device in the other 10 recordings (6 pigs; 117 min total duration; 11.7 ± 4.4 min per recording). Each mucosal recording period was paired with a simultaneous serosal reference recording such that total serosal recording duration was 222 min (105 min recorded simultaneously with the FPC electrode mucosal recordings, and 117 min recorded simultaneously with the modified Constellation™ device mucosal recordings). Slow-wave propagation was successfully and routinely mapped at the mucosal surface for both the FPC and modified Constellation™ devices, allowing for a comprehensive comparison of the slow-wave propagation and morphology between data recorded on the mucosal and serosal surfaces.

Slow-wave Propagation

Figure 2 shows representative slow-wave recordings mapped simultaneously from the serosal and mucosal surfaces using the FPC electrodes, while **Figure 3** shows comparison data recorded with the modified Constellation™ device. The activation maps for both devices in **Figures 2** and **3** show normal antegrade propagation sequences over the mucosal and serosal surfaces, consistent with known porcine gastric activation patterns.[21]

Gastric dysrhythmias were recorded in 6/8 pigs (7/10 recordings) during mucosal mapping with FPCs, and 3/6 pigs (6/10 recordings) during mucosal mapping with the modified Constellation™ device. Dysrhythmias included ectopic pacemakers, retrograde and circumferential propagation, conduction blocks, and colliding wavefronts, consistent with past studies.[2,3,20] An example dysrhythmia recorded by the FCP arrays simultaneously at the mucosal and serosal surfaces is presented in **Figure 4**. This dysrhythmia encompassed multiple cycles of retrograde propagation and wavelet rotation around a functional conduction block before being entrained by antegrade propagation, and activity occurred at abnormally low frequency of 1.4 ± 0.2 cpm across the recorded duration.

Slow-wave propagation dynamics were similar between the serosal and mucosal surfaces from all recordings, as determined by propagation animation and isochronal activation mapping. Propagation consistency was further verified by quantitative analysis of slow-wave

frequency and velocity compared between serosal and mucosal recordings (**Figure 5A,B**). Slow-wave frequencies were near-identical between serosa and mucosa for the FPC data (3.2 ± 0.2 vs 3.2 ± 0.2 cycles per minute (cpm); P=0.7) and the modified Constellation™ device (3.6 ± 0.1 vs 3.6 ± 0.1 cpm; P=0.3). Velocity calculations were also closely comparable between serosa and mucosa for the FPC (7.1 ± 0.7 vs 7.7 ± 0.7 mm s^{-1}; P=0.4) and modified Constellation™ device (6.0 ± 0.5 vs 6.3 ± 0.8 mm s^{-1}; P=0.8). These data support consistent detection of individual events, with consistent propagation profiles of grouped cycles, across both gastric surfaces and for both devices.

However, the mapped coverage (i.e., percent of electrodes that obtained slow wave signals) from the FPC arrays was 23% lower on average from the mucosa than the serosa (P=0.001), reflecting a reduced signal quality at the mucosal surface (**Figure 2E**). Most of the reduced contact occurred at the peripheries of the FPC arrays, indicating that incomplete electrode contact was a likely cause. Mapped coverage from the modified Constellation™ device on the mucosa was 38% lower on average than from the serosal reference FPC arrays (P<0.001). However, the modified Constellation™ device had a much different electrode array design than the FPCs, and covered the entire gastric circumference including the lesser curvature, which is known to be quiescent in the porcine stomach and thereby decreased the effective mapped coverage of the modified Constellation™ device.[21] Comparatively, the reference serosal FPC arrays only covered a portion (approximately 25%) of the circumference, and were positioned near the electrically active greater curvature.

Slow-wave Morphology

Slow-waves recorded from the mucosal surface were markedly attenuated compared to the reference serosal signals, with 72% lower amplitude from the FPC device (0.4 ± 0.1 vs 1.5 ± 0.2 mV; P<0.001) and 65% lower amplitude from the modified Constellation™ device (0.5 ± 0.1 vs 1.4 ± 0.2 mV; P<0.001) (**Figure 5C**). Slow-waves recorded from the mucosal surface also showed a slower activation profile, with an 18% wider downstroke compared to serosal recordings for the FPC electrodes (0.8 ± 0.04 vs 0.7 ± 0.03 s; P=0.02) and 31% wider for the modified Constellation™ device (0.8 ± 0.03 vs 0.6 ± 0.02 s; P=0.002) (**Figure 5D**). Together, these differences in amplitude and downstroke width combined to yield a mucosal downstroke gradient that was 75% lower from the FPC device compared to the reference serosal signals (0.5 ± 0.1 vs 2.1 ± 0.4 mV s^{-1}; P<0.001), and 73% lower from the modified Constellation™ device (0.7 ± 0.1 vs 2.4 ± 0.3 mV s^{-1}; P<0.001).

Signal morphology is compared in **Figure 6**, which shows average slow-wave morphology from 100 representative signals from each recording modality. The serosal slow-wave signals demonstrated the standard biphasic extracellular slow-wave morphology,[29] with a small initial sharp positive phase, followed by a rapid negative phase, before recovery to baseline in two phases (an initial sharp deflection before gradual return to baseline). The attenuated mucosal signals maintained the biphasic morphology, but occurred with decreased amplitude, wider downstroke, and loss of the smaller sharp deflections. However, the PCC calculations identified high positive correlation between all signal morphologies (0.95 for serosal FPC vs mucosal FPC; 0.94 for serosal FPC vs mucosal Constellation™;

0.99 for mucosal FPC versus mucosal Constellation™), suggesting close similarity in the important downstroke activation-phase of the signals.

Discussion

The emerging clinical translation of HR electrical mapping is proving a major advance in understanding gastric dysrhythmias, enabling the accurate identification, analysis, and classification of slow-wave initiation and conduction abnormalities.[2,3,10] However, human studies and clinical translation of this technology have been critically limited by the necessity for general anesthesia and surgical access to the gastric serosa. This study represents an important advance in HR mapping by demonstrating the feasibility of spatiotemporal slow-wave mapping from the mucosal surface, including during dysrhythmias, providing significant impetus to the development of clinically applicable mucosal mapping technology.

This study demonstrated the feasibility of HR gastric electrical mapping using two different electrode array types, with reference to serosal mapping data from validated methods.[12,29] Importantly, data mapped at the mucosal surface in this study was found to be consistent with serosal data, in terms of frequency, velocity, and propagation pattern, including for dysrhythmic cases. This finding is important, because the large volume of HR mapping data that has been accrued in recent years was all performed serosally, including descriptions of normal activation patterns,[15,30] dysrhythmia classifications,[2,20] and surgical and therapeutic interventions.[31,32] This existing body of literature can now be directly translated to aid interpretation of data recorded from the mucosal surface, including for both low- and high-resolution recordings. Interestingly, dysrhythmias were more prevalent in this study than in past porcine studies,[20] likely a consequence of the additional surgical intervention and handling associated with the intra-gastric incision in this study,[31] although potential effects from the intra-gastric balloon inflation should also be further investigated in the future.

Furthermore, this study has provided a quantitative foundation for mucosal mapping and has identified key differences in signal morphology between serosal and mucosal recordings, which will inform the future design of electrodes and devices, with a focus on improving mucosal signal quality. Data recorded from the mucosa in this study had substantially lower amplitude than serosal data (65-72%), with a slower downstroke (18-31%) and attenuated signal morphology, likely a consequence of the passive electrical properties of the mucosal tissue between the source and electrode, essentially serving as a low-pass filter, although further investigation of the electrophysiological mechanism is now required. These effects may render mucosal signal recognition challenging in the human gastric corpus using current methods, because human corpus slow-wave activity has a weaker amplitude than that of pigs.[15,21] A suitably high signal-to-noise ratio (SNR) and sharp downstroke are key morphological signatures for the reliable application of automated slow-wave analysis algorithms, which make efficient multi-electrode data throughput possible.[24,25,33] These methods were not suitable for the mucosal data in this study. However, now that this study has established foundational data for HR mucosal mapping, analytical algorithms and software could also be modified specifically for improvement of mucosal analysis in the future, for example by introducing noise-removal algorithms or optimizing detection

parameters for the specific mucosal signal morphology, as has been achieved for lower-SNR intestinal serosal slow-waves.[34–36] New algorithms for calculating velocity fields from non-uniform electrode grids will also be necessary in the future. For this study, velocity calculations from the modified Constellation™ device were performed assuming a uniform inter-electrode spacing of 11.4 mm, calculated as a representative global average uniform spacing between the 7 mm linear spacing along each spline of the device and the variable, larger circumferential spacing. In future, specific algorithms for calculating velocity profiles from three-dimensional, non-uniform electrode grids will enable more accurate characterization of slow wave propagation from the mucosal surface.

In addition to improvements in detection algorithms, it is likely that advances in electrode design could also help optimize mucosal HR gastric mapping. Improving electrode recordings requires the careful consideration of several factors, including biocompatibility, material properties, charge-transfer, signal stability, ease of use, and sterilization.[14,37] While FPCs have been a highly successful HR recording platform, including in human clinical studies, previous attempts to improve the SNR of FPCs by altering their electrode contact material yielded no difference in amplitude or SNR.[38] Therefore, new electrode designs may likely be required to improve mucosal signal quality, for example increased electrode contact area or protruding electrodes. Other advances will also be needed to miniaturize the arrays to allow delivery of the device through standard endoscopic ports and develop more flexible material to allow optimal placement through a curved endoscope. Integration of an anatomically-specific balloon design, like a tapered balloon to fit the decreasing circumference of the gastric antrum, could further improve signal acquisition and quality, and the effects of gastric distention by intra-gastric balloon inflation should be defined.

Potential alternative electrode design approaches can be informed by existing literature, where other investigators have achieved mucosal slow-wave recordings by low-resolution approaches. Monges and Salducci demonstrated excellent mucosal signal quality in single point recordings using a per-oral probe with a bipolar electrode pair placed within a rubber suction cup,[16,39] and approaches inspired by this method have been successfully adapted by other investigators.[19,40] Coleski and Hasler also successfully performed mucosal slow-wave recordings from a consecutive series of linear points in humans, using bipolar electrodes secured with endoclips.[17,41,42] Another approach, employed by Abell and colleagues, involves the placement of electrodes originally designed as cardiac pacing leads, which could be screwed into the mucosa at endoscopy and held in place with endoclips to enable mucosal slow wave recordings over several days, with successful application in conjunction with temporary gastric electrical stimulation.[9,18,43]

While the above approaches indicate that improving mucosal signals is feasible, their direct translation is not feasible for HR mapping, because the individual placement of many electrodes by these methods as a dense, uniformly-distributed field is impractical. A further important step in this study was therefore to also introduce an electrode array and deployment system that would be suitable for endoscopic HR gastric mapping, by adapting an existing minimally-invasive 64-channel electrophysiological device, the Constellation™ Mapping Catheter (Boston Scientific, MN), which is widely applied in cardiology.[44] This device was readily deployable via an esophagostomy, and was modified by inclusion of an

inflatable balloon to achieve and maintain sufficient mucosal contact, a key aspect for recording the relatively low-amplitude mucosal slow-wave events. At endoscopy, such a device could be placed with visual guidance, and endoscopic suction applied to collapse the gastric lumen and improve mucosal contact with the device. Based on the results of this study, other existing approaches for minimally-invasive mapping in electrocardiology could also warrant evaluation as potentially suitable techniques for gastric mapping, including non-contact mapping.[13]

The primary method of non-invasive slow-wave recording remains electrogastrography (EGG), where electrodes are placed on the body-surface.[6] These methods benefit from their non-invasive approach, but are prone to low signal-to-noise ratio and difficulties in interpretation. As such, analyses of EGG signals have generally been restricted to frequency-based methods,[8] ignoring the accuracy and spatial information necessary for the reliable characterization and diagnosis of spatially complex gastric dysrhythmias,[9] many of which have been observed to occur within the normal frequency range.[2] This study has demonstrated that endoscopic mucosal mapping can provide a minimally-invasive approach capable of recording the necessary complex spatiotemporal slow-wave information and providing results consistent with those obtained by the highly-accurate but surgically-invasive serosal mapping.

In conclusion, this study demonstrates the feasibility of HR endoscopic mucosal slow-wave mapping and provides a quantitative foundation for the further development and human translation of this technology. These results now enable further investigation into improved electrode design, data analysis algorithms, and endoscopically-deliverable devices to enable endoscopic mapping to achieve clinical translation as a tool to investigate and diagnose gastric dysrhythmias.

Acknowledgements

We thank Linley Nisbet for her expert technical assistance.

Funding

This work and/or authors were supported by the Medical Technologies Centre of Research Excellence (MedTech CoRE) New Zealand, Health Research Council of New Zealand, and the National Institutes of Health (R01 DK64775, R01 DK57061).

Abbreviations

ICC	interstitial cells of Cajal
HR	high-resolution
FPC	flexible-printed-circuit
AT	activation time
GEMS	Gastrointestinal Electrical Mapping Suite (software)
PCC	Pearson correlation coefficient

cpm	cycles per minute
SNR	signal-to-noise ratio

References

1. Huizinga JD, Lammers WJEP. ut peristalsis is governed by a multitude of cooperating mechanisms. Am J Physiol Gastrointest Liver Physiol. 2009; 296:G1–8. [PubMed: 18988693]
2. Angeli TR, Cheng LK, Du P, Wang TH-H, Bernard CE, Vannucchi M-G, et al. Loss of interstitial cells of Cajal and patterns of gastric dysrhythmia in patients with chronic unexplained nausea and vomiting. Gastroenterology. 2015; 149(1):56–66. e5. [PubMed: 25863217]
3. O'Grady G, Angeli TR, Du P, Lahr C, Lammers WJEP, Windsor JA, et al. Abnormal initiation and conduction of slow-wave activity in gastroparesis, defined by high-resolution electrical mapping. Gastroenterology. 2012; 143(3):589–98. e1–3. [PubMed: 22643349]
4. Grover M, Farrugia G, Lurken MS, Bernard CE, Faussone-Pellegrini MS, Smyrk TC, et al. Cellular changes in diabetic and idiopathic gastroparesis. Gastroenterology. 2011; 140(5):1575–85. e8. [PubMed: 21300066]
5. Lin X, Chen JZ. Abnormal gastric slow waves in patients with functional dyspepsia assessed by multichannel electrogastrography. Am J Physiol Gastrointest Liver Physiol. 2001; 280(6):G1370–5. [PubMed: 11352832]
6. Parkman HP, Hasler WL, Barnett JL, Eaker EY. Electrogastrography: a document prepared by the gastric section of the American Motility Society Clinical GI Motility Testing Task Force. Neurogastroenterol Motil. 2003; 15(2):89–102. [PubMed: 12680908]
7. O'Grady G, Wang T, Du P, Angeli TR, Lammers WJEP, Cheng LK. Recent progress in gastric arrhythmia: pathophysiology, clinical significance and future horizons. Clin Exp Pharmacol Physiol. 2014; 41(10):854–62. [PubMed: 25115692]
8. Bortolotti M. Electrogastrography: a seductive promise, only partially kept. Am J Gastroenterol. 1998; 93(10):1791–4. [PubMed: 9772032]
9. O'Grady G, Abell TL. Gastric arrhythmias in gastroparesis: low- and high-resolution mapping of gastric electrical activity. Gastroenterol Clin North Am. 2015; 44(1):169–84. [PubMed: 25667031]
10. Lammers WJEP, Ver Donck L, Stephen B, Smets D, Schuurkes JAJ. Focal activities and re entrant propagations as mechanisms of gastric tachyarrhythmias. Gastroenterology. 2008; 135(5):1601–11. [PubMed: 18713627]
11. Lammers WJEP. Arrhythmias in the gut. Neurogastroenterol Motil. 2013; 25(5):353–7. [PubMed: 23490042]
12. Du P, O'Grady G, Egbuji JU, Lammers WJEP, Budgett D, Nielsen P, et al. High-resolution mapping of in vivo gastrointestinal slow wave activity using flexible printed circuit board electrodes: methodology and validation. Ann Biomed Eng. 2009; 37(4):839–46. [PubMed: 19224368]
13. Shenasa, M.Hindricks, G.Borggrefe, M.Breithardt, G., Josephson, ME., editors. Cardiac Mapping. 4th ed.. Wiley-Blackwell; Oxford, UK: 2013.
14. O'Grady, G., Angeli, TR., Lammers, WJEP. The principles and practice of gastrointestinal high-resolution electrical mapping.. In: Cheng, LK., Farrugia, G., editors. New Advances in Gastrointestinal Motility Research. Springer Netherlands; Dordrecht: 2013. p. 51-69.
15. O'Grady G, Du P, Cheng LK, Egbuji JU, Lammers WJEP, Windsor JA, et al. Origin and propagation of human gastric slow-wave activity defined by high-resolution mapping. Am J Physiol Gastrointest Liver Physiol. 2010; 299(3):G585–92. [PubMed: 20595620]
16. Monges H, Salducci J. Electrical activity of the gastric antrum in normal human subjects. Am J Dig Dis. 1971; 16(7):623–7. [PubMed: 5563215]
17. Coleski R, Hasler WL. Coupling and propagation of normal and dysrhythmic gastric slow waves during acute hyperglycaemia in healthy humans. Neurogastroenterol Motil. 2009; 21(5):492–9. e1–2. [PubMed: 19309443]

18. Ayinala S, Batista O, Goyal A, Al-Juburi A, Abidi N, Familoni B, et al. Temporary gastric electrical stimulation with orally or PEG-placed electrodes in patients with drug refractory gastroparesis. Gastrointest Endosc. 2005; 61(3):455–61. [PubMed: 15758925]
19. Bortolotti M, Sarti P, Barbara L, Brunelli F. Gastric myoelectric activity in patients with chronic idiopathic gastroparesis. J Gastroint Motil. 1990; 2(2):104–8.
20. O'Grady G, Egbuji JU, Du P, Lammers WJEP, Cheng LK, Windsor JA, et al. High-resolution spatial analysis of slow wave initiation and conduction in porcine gastric dysrhythmia. Neurogastroenterol Motil. 2011; 23(9):e345–55. [PubMed: 21714831]
21. Egbuji JU, O'Grady G, Du P, Cheng LK, Lammers WJEP, Windsor JA, et al. Origin, propagation and regional characteristics of porcine gastric slow wave activity determined by high-resolution mapping. Neurogastroenterol Motil. 2010; 22(10):e292–300. [PubMed: 20618830]
22. Paskaranandavadivel N, O'Grady G, Du P, Cheng LK. Comparison of filtering methods for extracellular gastric slow wave recordings. Neurogastroenterol Motil. 2013; 25(1):79–83. [PubMed: 22974243]
23. Yassi R, O'Grady G, Paskaranandavadivel N, Du P, Angeli TR, Pullan AJ, et al. The gastrointestinal electrical mapping suite (GEMS): software for analyzing and visualizing high-resolution (multi-electrode) recordings in spatiotemporal detail. BMC Gastroenterol. 2012; 12(1): 60. [PubMed: 22672254]
24. Erickson JC, O'Grady G, Du P, Obioha C, Qiao W, Richards WO, et al. Falling-edge, variable threshold (FEVT) method for the automated detection of gastric slow wave events in high-resolution serosal electrode recordings. Ann Biomed Eng. 2010; 38(4):1511–29. [PubMed: 20024624]
25. Erickson JC, O'Grady G, Du P, Egbuji JU, Pullan AJ, Cheng LK. Automated gastric slow wave cycle partitioning and visualization for high-resolution activation time maps. Ann Biomed Eng. 2011; 39(1):469–83. [PubMed: 20927594]
26. Paskaranandavadivel N, Cheng LK, Du P, O'Grady G, Pullan AJ. Improved signal processing techniques for the analysis of high resolution serosal slow wave activity in the stomach. Conf Proc IEEE Eng Med Biol Soc. 2011; 2011:1737–40. [PubMed: 22254662]
27. Paskaranandavadivel N, O'Grady G, Du P, Pullan AJ, Cheng LK. An improved method for the estimation and visualization of velocity fields from gastric high-resolution electrical mapping. IEEE Trans Biomed Eng. 2012; 59(3):882–9. [PubMed: 22207635]
28. Goyal R, Harvey M, Daoud EG, Brinkman K, Knight BP, Bahu M, et al. Effect of coupling interval and pacing cycle length on morphology of paced ventricular complexes. Implications for pace mapping. Circulation. 1996; 94(11):2843–9. [PubMed: 8941111]
29. Angeli TR, Du P, Paskaranandavadivel N, Janssen PWM, Beyder A, Lentle RG, et al. The bioelectrical basis and validity of gastrointestinal extracellular slow wave recordings. J Physiol. 2013; 591(Pt 18):4567–79. [PubMed: 23713030]
30. Lammers WJEP, Ver Donck L, Stephen B, Smets D, Schuurkes JAJ. Origin and propagation of the slow wave in the canine stomach: the outlines of a gastric conduction system. Am J Physiol Gastrointest Liver Physiol. 2009; 296(6):G1200–10. [PubMed: 19359425]
31. Du P, Hameed A, Angeli TR, Lahr C, Abell TL, Cheng LK, et al. The impact of surgical excisions on human gastric slow wave conduction, defined by high-resolution electrical mapping and in silico modeling. Neurogastroenterol Motil. 2015; 27(10):1409–22. [PubMed: 26251163]
32. Angeli TR, Du P, Midgley D, Paskaranandavadivel N, Sathar S, Lahr C, et al. Acute slow wave responses to high-frequency gastric electrical stimulation in patients with gastroparesis defined by high-resolution mapping. Neuromodulation. 2016 Epub ahead of print.
33. Paskaranandavadivel N, O'Grady G, Cheng LK. Time-Delay Mapping of High-Resolution Gastric Slow-Wave Activity. IEEE Trans Biomed Eng. Jan; 2017 64(1):166–172. [PubMed: 27071158]
34. Angeli TR, O'Grady G, Paskaranandavadivel N, Erickson JC, Du P, Pullan AJ, et al. Experimental and automated analysis techniques for high-resolution electrical mapping of small intestine slow wave activity. J Neurogastroenterol Motil. 2013; 19(2):179–91. [PubMed: 23667749]
35. Erickson JC, Putney J, Hilbert D, Paskaranandavadivel N, Cheng LK, O'Grady G, et al. Iterative covariance-based removal of time-synchronous artifacts: application to gastrointestinal electrical recordings. IEEE Trans Biomed Eng. 2016; 63(11):2262–2272. [PubMed: 26829772]

36. Erickson JC, Velasco-Castedo R, Obioha C, Cheng LK, Angeli TR, O'Grady G. Automated algorithm for GI spike burst detection and demonstration of efficacy in ischemic small intestine. Ann Biomed Eng. 2013; 41(10):2215–28. [PubMed: 23612912]

37. McAdams, E. Bioelectrodes.. In: Webster, JG., editor. Encyclopedia of Medical Devices and Instrumentation. 2nd ed.. Wiley; New York: 2006. p. 120-66.

38. O'Grady G, Paskaranandavadivel N, Angeli TR, Du P, Windsor JA, Cheng LK, et al. A comparison of gold versus silver electrode contacts for high-resolution gastric electrical mapping using flexible printed circuit board arrays. Physiol Meas. 2011; 32(3):N13–22. [PubMed: 21252419]

39. Monges H, Salducci J. A method of recording the gastric electrical activity in man. Am J Dig Dis. Mar; 1970 15(3):271–6. [PubMed: 5435946]

40. You CH, Lee KY, Chey WY, Menguy R. Electrogastrographic study of patients with unexplained nausea, bloating, and vomiting. Gastroenterology. 1980; 79(2):311–4. [PubMed: 7399235]

41. Coleski R, Hasler WL. Directed endoscopic mucosal mapping of normal and dysrhythmic gastric slow waves in healthy humans. Neurogastroenterol Motil. 2004; 16(5):557–65. [PubMed: 15500512]

42. Coleski R, Hasler W. Regional gastric slow wave propagation and coupling measured by endoscopy-directed multichannel gastric mucosal recording in healthy humans: effects of acute hyperglycemia. Neurogastroenterol Motil. 2006; 18:740.

43. Abell TL, Johnson WD, Kedar A, Runnels JM, Thompson J, Weeks ES, et al. A double-masked, randomized, placebo-controlled trial of temporary endoscopic mucosal gastric electrical stimulation for gastroparesis. Gastrointest Endosc. 2011; 74(3):496–503. e3. [PubMed: 21872708]

44. Pappone C, Santinelli V. Multielectrode basket catheter: a new tool for curing atrial fibrillation? Heart Rhythm. 2006; 3(4):385–6. [PubMed: 16567282]

Key Points

- High-resolution electrical mapping has advanced the accurate assessment of gastric dysrhythmias, offering promise as a diagnostic technique, but has been restricted to invasive surgical access to date. This study investigated high-resolution electrical mapping from the gastric mucosal surface as feasibility for endoscopic gastric electrical mapping.
- Slow-wave activity was consistently recorded from the mucosal surface, and propagation was consistent with reference serosal activation pattern, frequency, and velocity, including during dysrhythmias. However, mucosal waveforms exhibited reduced amplitude and wider downstroke width.
- This study demonstrates feasibility of endoscopic high-resolution mapping, providing a foundation for advancement of minimally-invasive spatiotemporal gastric mapping as a clinical and scientific tool.

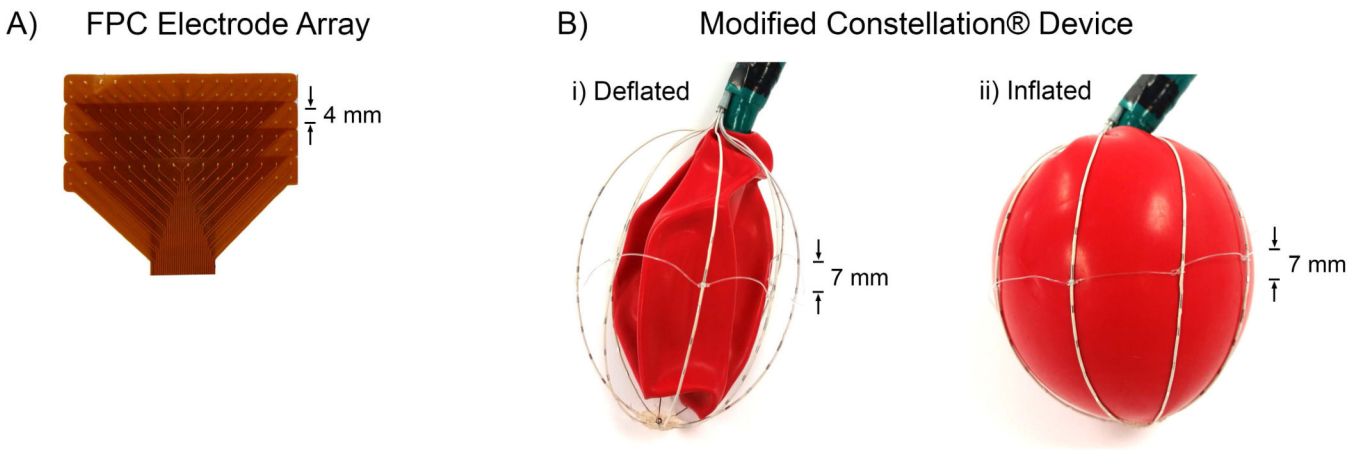

Figure 1.

Electrode arrays. **A)** FPC electrode array encompassing 128 total electrodes, arranged in a 16 x 8 array, with 4 mm inter-electrode spacing. This FPC array was used for all serosal reference recordings in this study, and a second identical array was used for FPC mucosal recordings. **B)** Modified Constellation™ electrode array for mucosal mapping encompassing 64 total electrodes arranged in a flexible 'basket' (75 mm diameter) of 8 vertical strands. Each strand encompassed 8 electrodes with 7 mm inter-electrode spacing. An internal balloon was built into the middle of the basket, enabling deflation of the device (*i*) for induction into the stomach, and inflation of the device (*ii*) to achieve and maintain electrode contact with the mucosal surface during recording periods.

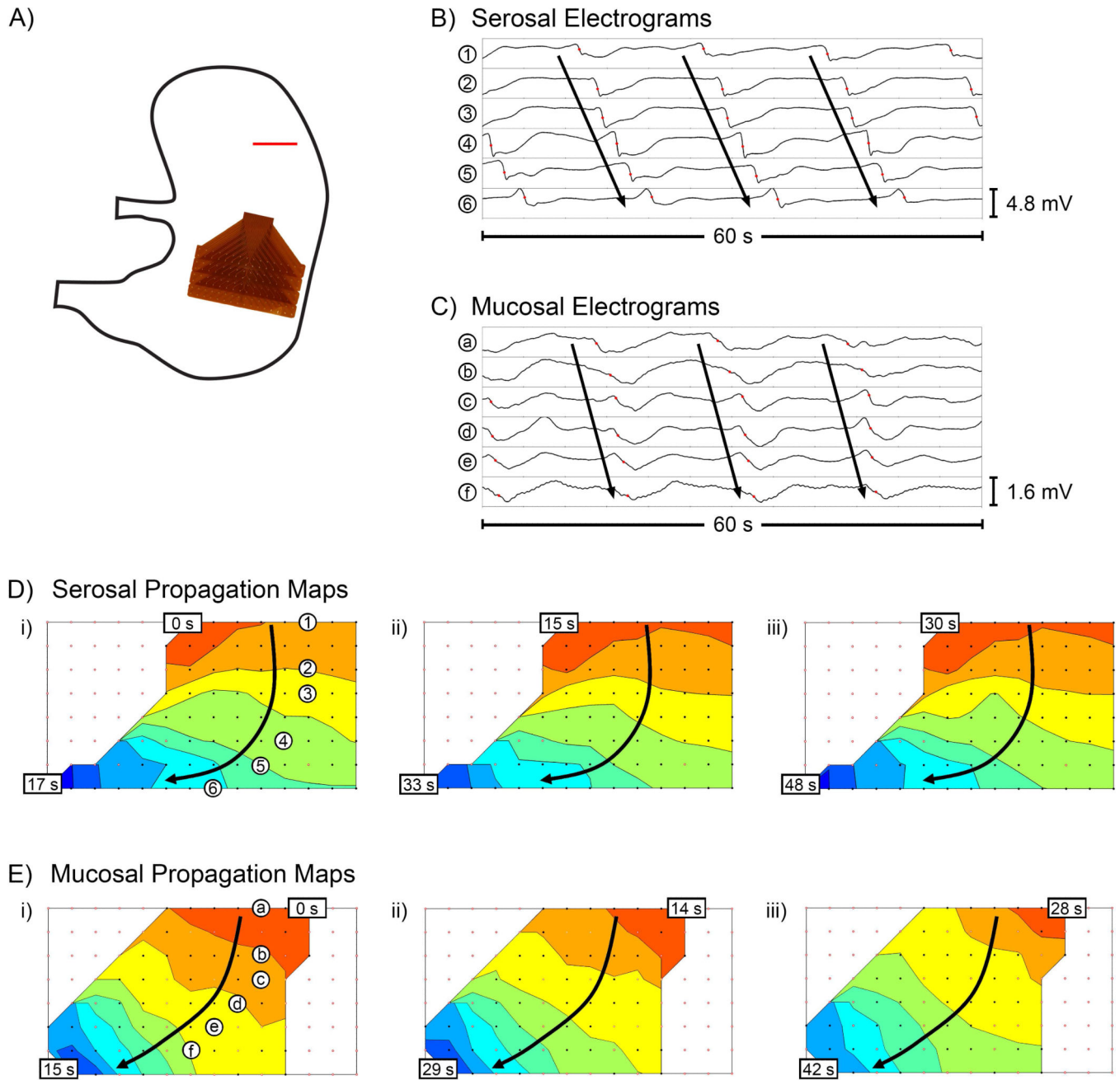

Figure 2.

Comparison of normal antegrade slow-wave propagation simultaneously mapped from the serosal and mucosal surfaces using FPC electrode arrays. **A)** FPC electrode arrays were placed in direct opposition on the mucosa and serosa of the mid-corpus; red line indicates position of incision through gastric wall. **B,C)** Electrograms from the serosa (*B*) vs mucosa (*C*) from corresponding electrode positions as labeled in panels *Di* and *Ei*, respectively. **D,E)** Isochronal activation maps of slow-wave propagation from the serosa (*D*) vs mucosa (*E*), across successive waves (*i-iii*). Slow-wave propagation was consistent between mucosal and serosal recordings. Black dots represent electrodes, with white dots outlined in red

representing electrodes where activity was interpolated. Each color band (‘isochrone’) shows the area of slow-wave propagation per 2 s, from red (early) to blue (late).

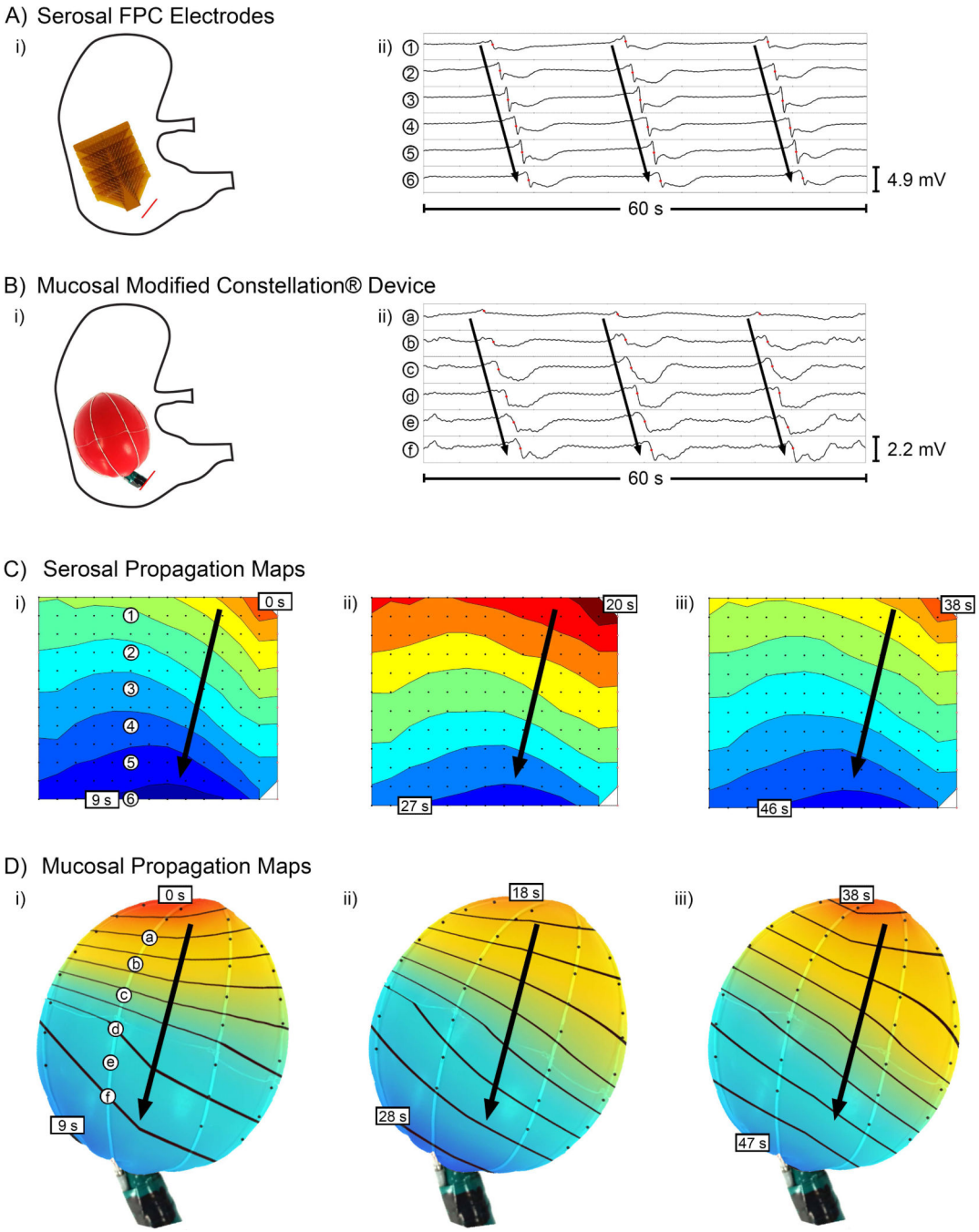

Figure 3.

Comparison of normal antegrade slow-wave propagation simultaneously mapped from the serosa with FPC electrodes and mucosa with a modified Constellation™ electrode array. **A)** Position of serosal FPC electrode array (*i*, red line indicates position of incision through gastric wall) and electrograms (*ii*) from corresponding electrode positions labeled in panel *Ci*. **B)** Position of mucosal modified Constellation™ electrode array (*i*) and electrograms (*ii*) from corresponding electrode positions labeled in panel *Di*. **C,D)** . Isochronal activation maps of slow-wave propagation recorded simultaneously from the serosal FPC electrodes

(*C*) vs mucosal modified Constellation™ (*D*), across successive waves (*i-iii*). Slow-wave propagation was consistent between mucosal and serosal recordings. Activation maps are as described in Figure 2, with 1 s isochrones.

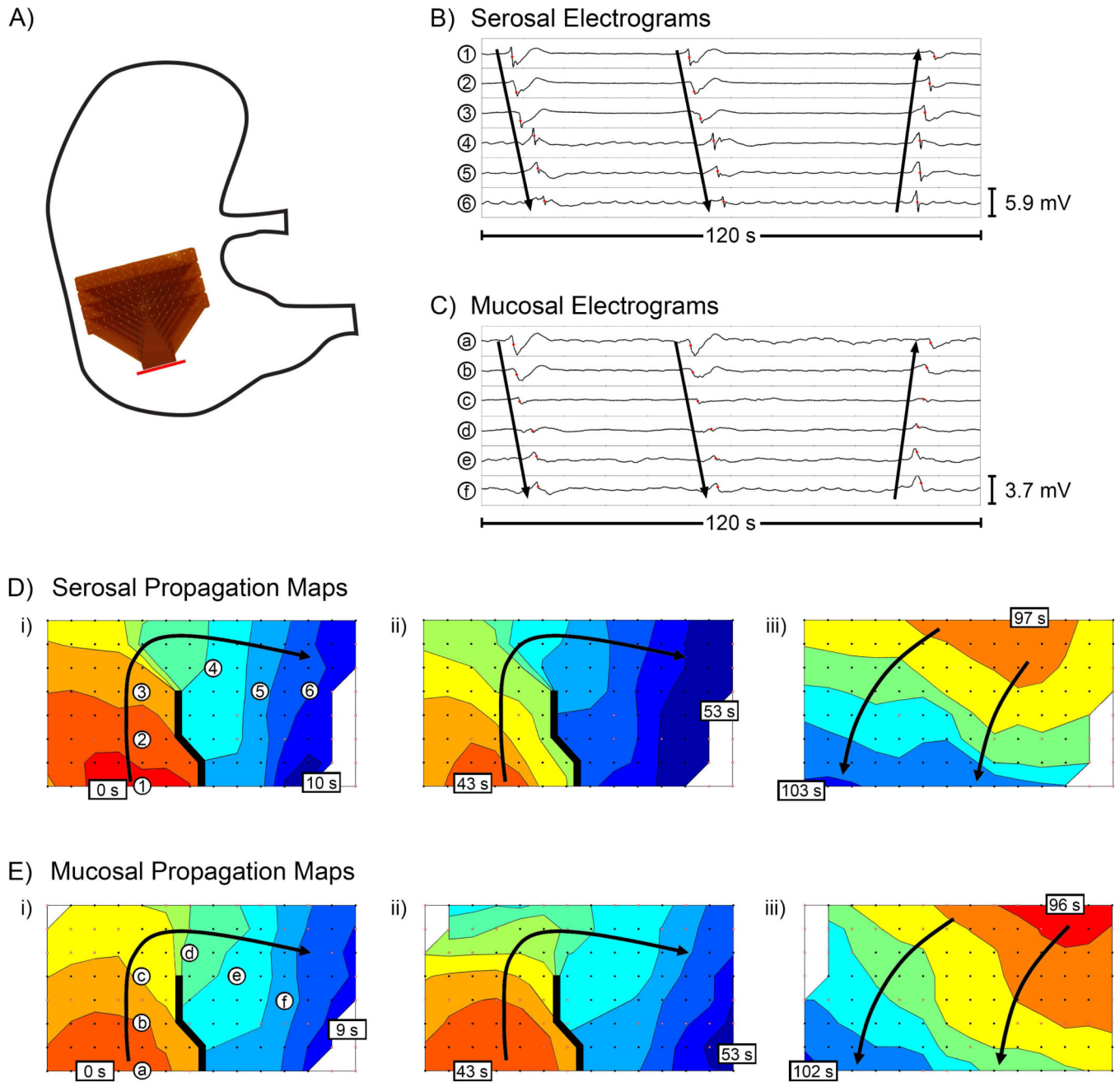

Figure 4.

Comparison of dysrhythmic slow-wave propagation simultaneously mapped from the serosal and mucosal surfaces using FPC electrode arrays. **A)** FPC electrode arrays were placed in direct opposition on the mucosa and serosa of the corpus; red line indicates position of incision through gastric wall. **B,C)** Electrograms from the serosa (*B*) vs mucosa (*C*) from corresponding electrode positions as labeled in panels *Di* and *Ei*, respectively. **D,E)** Isochronal activation maps of slow-wave propagation from the serosa (*D*) vs mucosa (*E*), across successive waves (*i-iii*). Slow-wave propagation was consistent between mucosal and serosal recordings. Shown here are two cycles of dysrhythmic slow-wave propagation

encompassing retrograde propagation and wavelet rotation around a functional conduction block represented by a thick black line (i, ii), followed by a cycle of antegrade propagation (iii). Activation maps are as described in Figure 2, with 1 s isochrones.

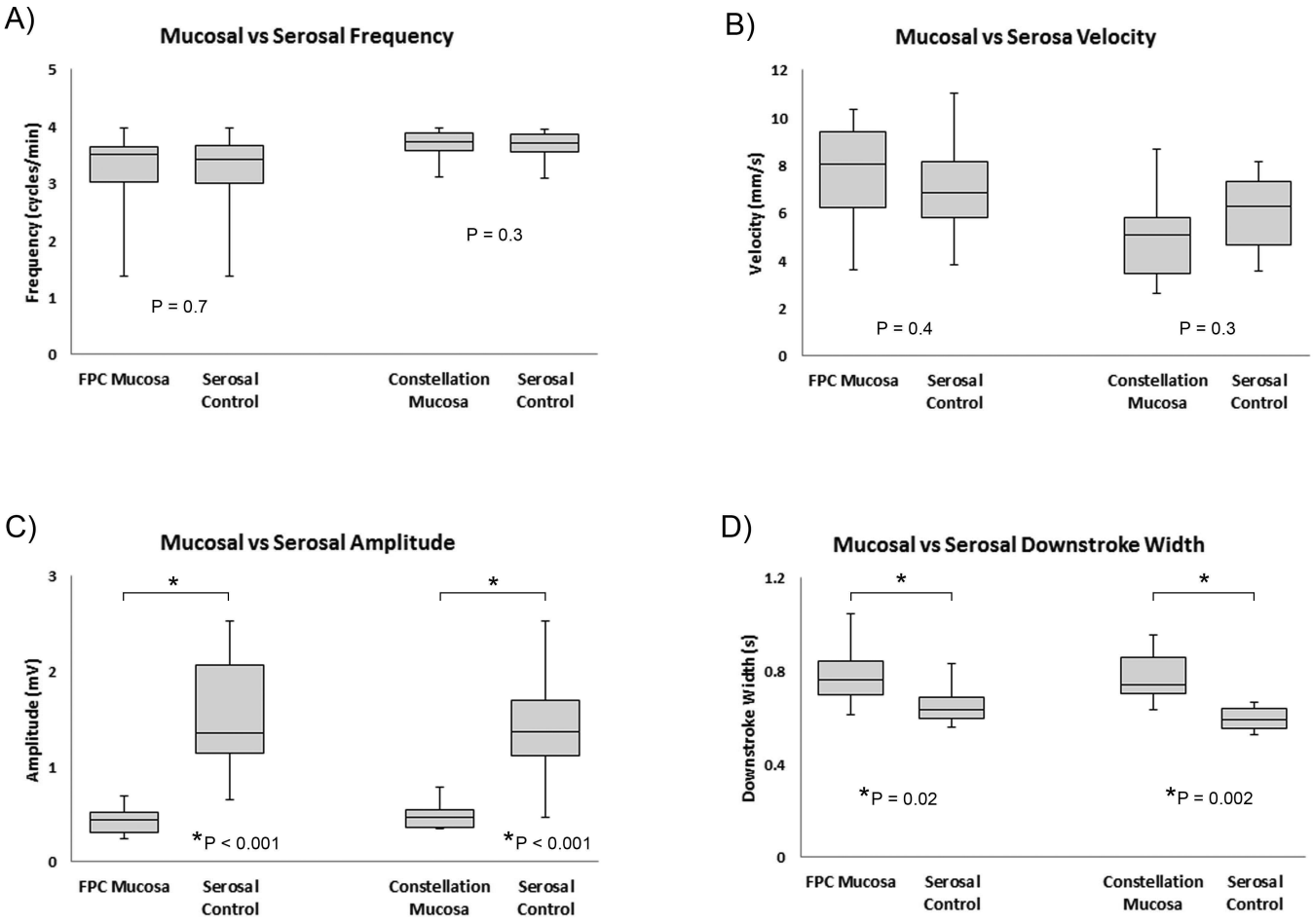

Figure 5.

Comparison of quantitative slow-wave characteristics between serosal vs mucosal recordings, including: **A)** Frequency; **B)** Velocity; **C)** Amplitude; and **D)** Downstroke width.

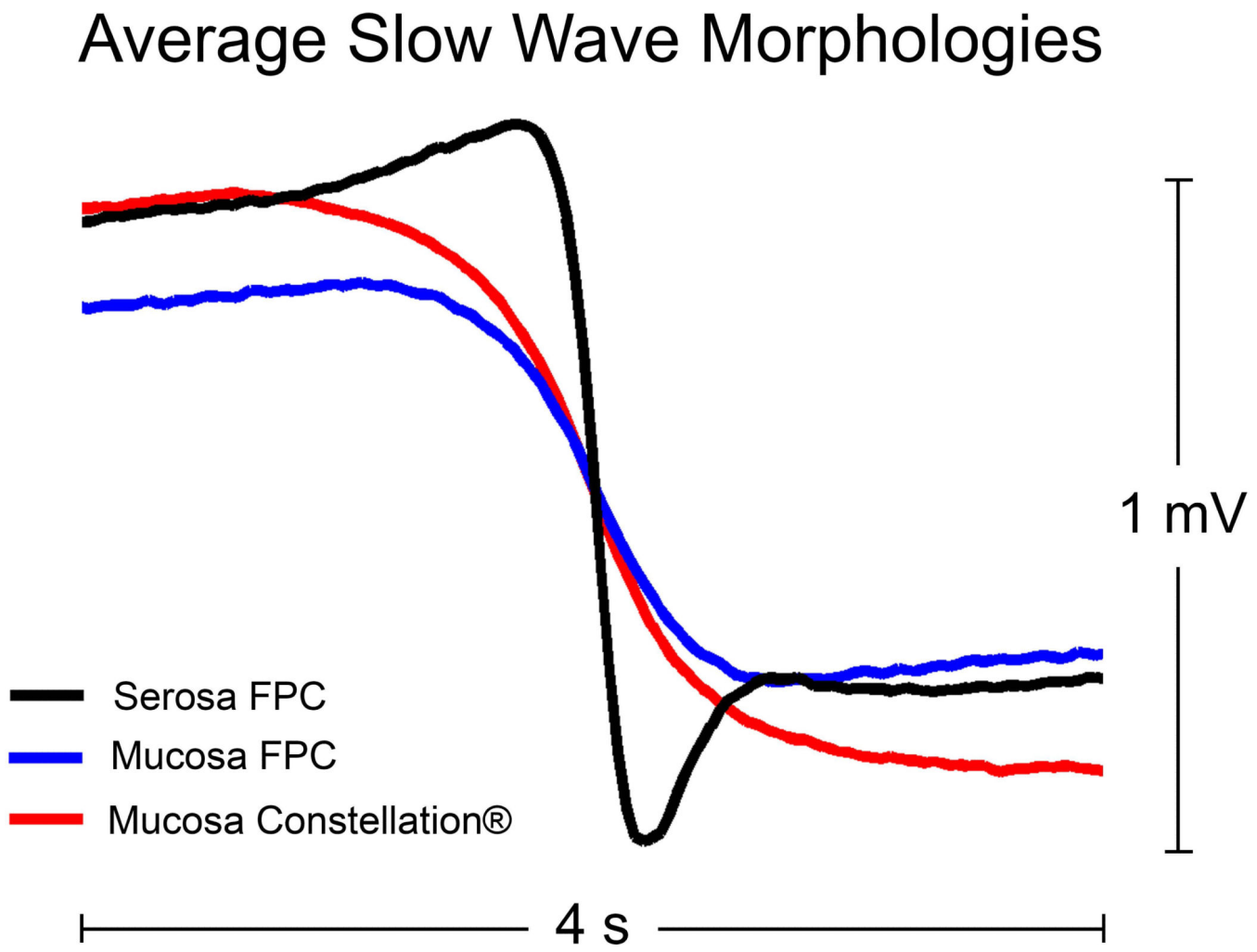

Figure 6.

Average slow-wave morphologies from the reference serosal FPC electrode arrays versus mucosal FPC and modified Constellation™ electrode arrays, demonstrating the decreased amplitude and wider downstroke achieved from the mucosal surface.